Designing for Static and Dynamic Loading of a Gear Reducer Housing with FEA

M. Davis, Y.S. Mohammed, A.A. Elmustafa, P.F. Martin and C. Ritinski

Management Summary

A recent trend has been a movement to more user-friendly products in the mechanical power transmission industry. A good example of such a product is a high-horsepower, right angle, shaft-mounted drive designed to minimize installation efforts. Commonly referred to as an alignment-free type, it allows the drive package mounting to be quicker, more cost effective and require less expertise during installation. This facilitates the use of the drive in applications such as underground mining, where there is little room to maneuver parts. The most common application for the alignment-free style drive is for powering bulk material handling belt conveyors.

An alignment-free drive is direct-coupled to the driven shaft only; it is not firmly attached to a foundation or rigid structure. A connecting link or torque arm connects the drive to a fixed structure, which limits the drive's rotational movement about the driven shaft. The electric motor is supported by the reducer housing through a fabricated, steel motor adapter; the coupling connecting the motor shaft and reducer shaft is enclosed by this motor adapter.

Sumitomo Drive Technologies is working on a design of the alignment-free system by using finite element analysis (FEA) to help guide the design process. FEA was used to test the cast iron housing to determine any potential problem areas before production begins. Once analyses were completed, the motor adapter was redesigned to lower stresses using the information from the FEA and comparing it to field test data.

Introduction

Sumitomo Drive Technologies' goal is to maximize the use of standard products and to expand this design philosophy to applications beyond underground mining.

Gear reducers allow electric motors producing relatively small torque to create high output torque through a series of gears (Refs. 1–4). The weight of both the motor and reducer, plus the movement of the complete drive assembly, can create high stresses on the interface between the reducer and the motor or motor adapter. Motor-induced vibrations due to gear meshing, etc., also play a significant role in reducer analysis. (Refs. 5–10). These vibrations are greater at start-up, and can produce large dynamic forces and torques that increase the risk of gear reducer housing failure at the interface with the motor adapter. In order to determine if the current reducer design meets the requirements of the proposed alignment-free drive systems, the reducer housing was analyzed under both static and dynamic loads using FEA. Pertinent results, structure optimization proposals, and conclusions are introduced in the following sections.

FEA of Gear Reducer Housing

FEA modeling. In order to simulate the system effectively, the entire system was analyzed as an assembly. Based on an existing and operating prototype design, the alignment-free drive was modeled in *Autodesk Inventor*. Figure 1 shows the entire assembly. The drive is connected to the motor adapter, which varies in size depending on what type and model of coupling it houses. The motor is also connected to the motor adapter on the right side by a series of bolts.

The solid model was converted to a step file (.stp) and imported into *PTC Pro/Mechanica*.

The FEA model was meshed in *Pro/Mechanica* using p-type elements, and a simple linear analysis was performed. Bolts were modeled using *Pro/Mechanica's* fastener application. This method simulates the bolt as a spring element passing through the two fastened parts. The load is completely transferred through the bolt rather than the touching components. The entire assembly mesh is shown in Figure 2. The FEA model had a maximum of 133,812 elements. Although this assembly is very large, it was simplified by removing many structurally insignificant features. Analyzing the entire system (reducer housing, coupling box and motor) as an assembly made it very complicated to simulate. More complexity in the model, in terms of features, means more elements and hence less accuracy. Significant effort was made to simplify the model while maintaining the structural properties of the system.

Both the static and dynamic analyses were conducted in this environment. The loads applied are the weight of the entire system and the torque reaction due to the action of the output shaft. The initial torque on the system at startup is about 300% of the rated torque. This factor of three has been taken into account while applying the loads. The alignment-free system is designed to be both flippable and reversible. The term "flippable" describes the reducer's capability of operating in both right-side-up and upside-down positions. "Reversible" refers to the reducer's ability to operate in both CW and CCW shaft rotations. Analysis of the housing was done in such a way as to test with the torque applied in both the clockwise and counterclockwise direction on the output shaft.

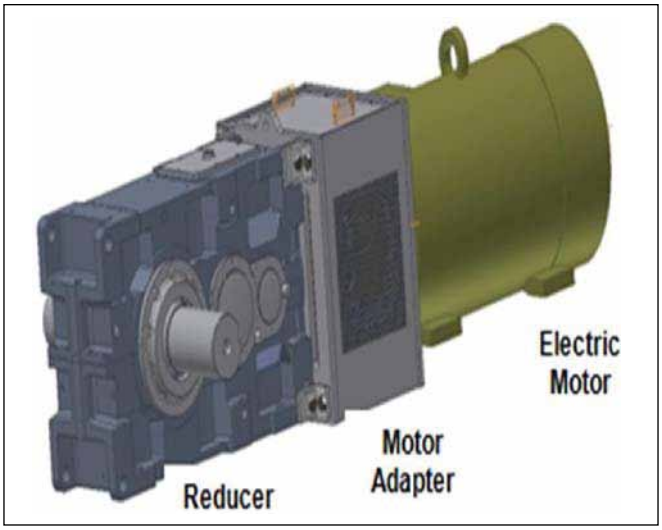

Figure 1—Alignment-free drive system.

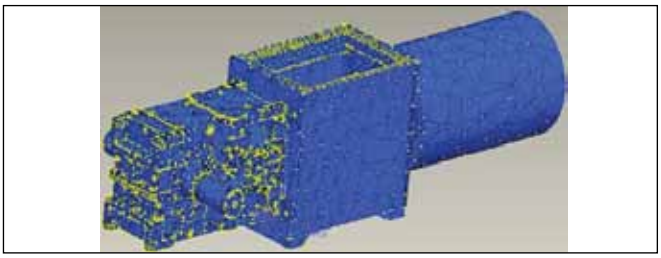

Figure 2—FEA model mesh.

Figure 3—Bracket and bracket located on housing.

The reducer housing is typically made of cast iron. The motor adapter is made of plates of A36 and structural tubing. This design allows the motor adapter to be relatively lightweight. Both the top and the bottom of the adapter have a cover plate that can be quickly and easily taken off for access to the coupling. The reducer housing and the coupling box are bolted together. Figure 3 shows corner brackets that were put in place as additional support, if needed. These corner brackets were included on the prototype units, pending confirmation of the housing strength analysis.

Static analysis. The reducer housing is connected to the rest of the assembly by four bolts at the high-speed, end-face of the housing. Besides the bolts there is also a fail-safe device in the form of brackets at the four corners of the end-face of the housing. As a conservative approach, static analyses were conducted with and without the brackets. The free-body diagram of the entire drive system is given in Figure 4, and it details how the loads were applied.

The stress without the brackets was high, but not fatal. With the brackets, however, the stress was reduced considerably. Figure 5 shows the stress distribution around the bolt holes of the reducer interface. The stress distribution on the

continued

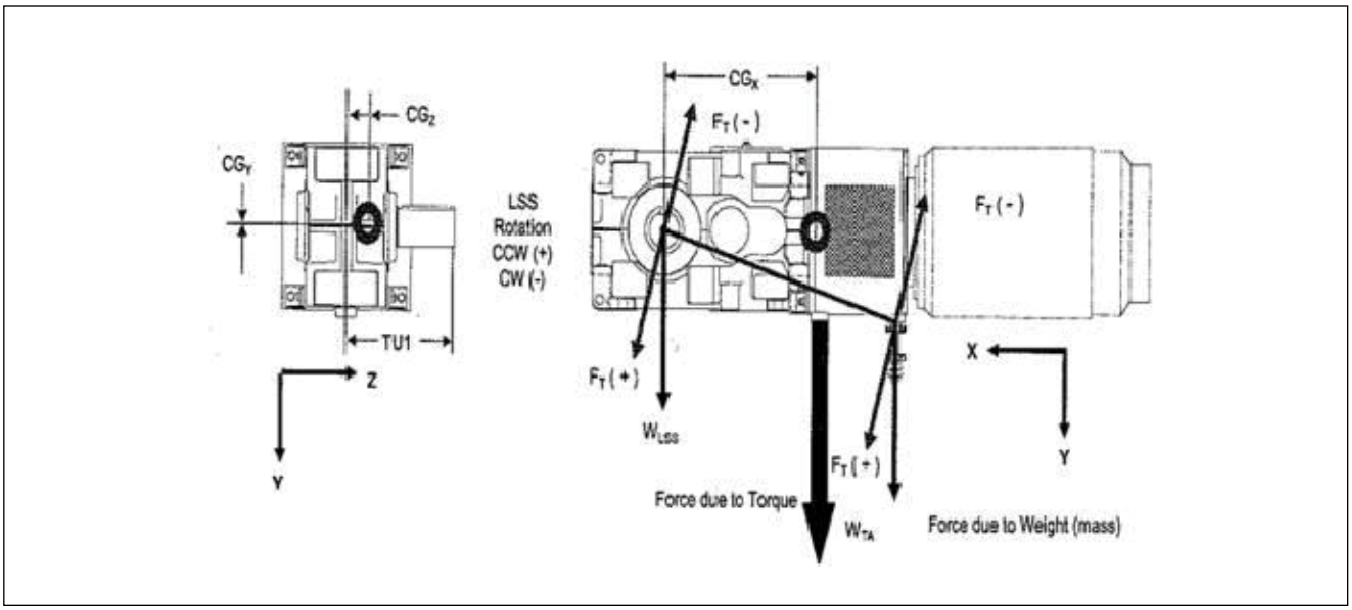

Figure 4—Free-body diagram.

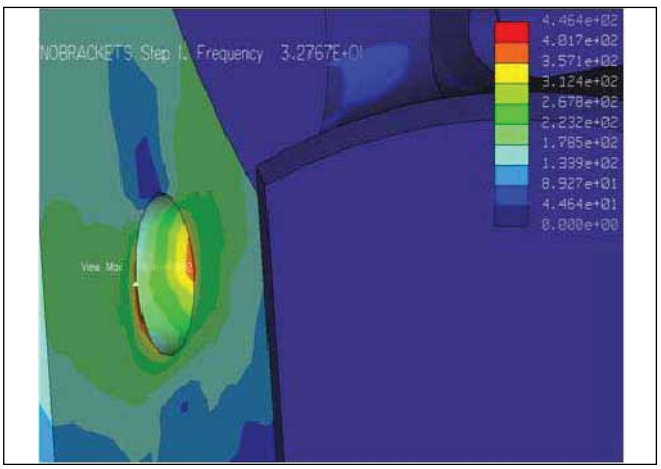

Figure 5—Stress distribution on reducer interface.

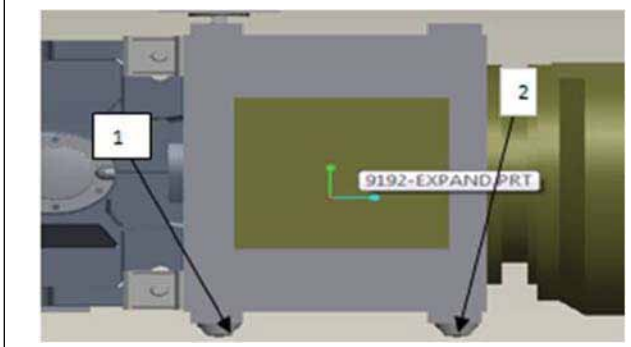

Figure 6—Torque arm positions.

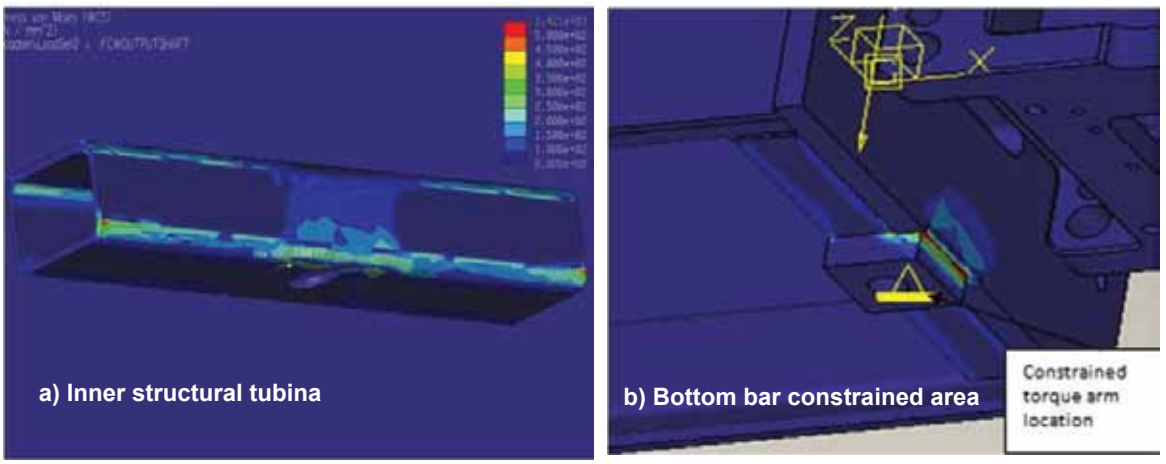

Figure 7—Static analysis stress field.

rest of the housing shows the area of high stresses.

Many of the high-stress areas are the sharp edges and holes. Higher stresses are due to the stress concentration in the area where the geometry is smaller and thinner. These are the particular areas of concern. Two cases arise as a result of variable torque arm location (Fig. 6)—(1) the torque arm is designed in such a way as to only allow slight movement in the negative Y-direction (Fig. 4); and (2) when the loads associated with a counterclockwise output shaft rotation are applied, the reducer is forced down on the torque arm, allowing no further movement along the Y-direction.

With the model constrained at the torque arm location (Ref. 1; Fig. 6) with zero degrees of freedom in every direction, high stresses were seen on the structural tubing in Figure 7a. This tubing and the area surrounding show stresses above failure. Figure 7a shows that stress concentration in two major areas—the circular mounting hole and the round corners of the structural tubing. The maximum stress on the structural tubing is 543 MPa, and it occurred on the outermost edges of the exterior of the tubing. This stress concentration area is very small and should be omitted due to stress singularities at those points.

A local maximum stress occurred near the edge of the mounting hole of 400 MPa. Because A36 steel tubing has an ultimate tensile strength of around 450 MPa, this stress could cause the tubing to yield. With the weight of the system, and the external torque applied, the structural tubing of the motor adapter could fail in those areas of high stress.

Figure 7b shows the mounting hole that was constrained during the analysis. High stresses were seen on the edge of this mounting bar, due to a pinching effect. When the loads are applied while that location is held fixed, a significant amount of bending stress is created in the area where the mounting bar meets the structural tubing and outermost motor plate (Fig. 7b). The local maximum stresses of this outermost plate are around 200 MPa, and therefore will not cause failure.

Similar analyses were conducted with counterclockwise torque and the two locations of the torque arm. These analyses, however, showed lower stresses and were disregarded. In this way, a worst-case loading scenario was obtained.

In the static analysis, the plate at this interface—between the motor adapter and the reducer box—exhibited much higher stresses than the reducer, and is thereby the limiting factor of the design. The greater thickness of the reducer housing at the interface allowed that area to produce little stress.

In order to get lower stresses, many of the parts were redesigned in an iterative process. The plates and structural tubing were thickened, but the stresses were still high and the cost of these modifications would increase the production cost. Eventually, the solution that proved to be easy and cost-effective in terms of manufacturing was to extend the bottom bar to the entire width of the coupling box. This causes the reaction forces from the torque arm to act over the entire coupling box instead of a small region, thereby lowering the stresses.

Figure 8 shows the results from the static analysis with the extended bar. With this bar extended, the stresses were around 60 MPa. These stresses were located on the bar mounting hole. With this small modification, a significant reduction in stresses was achieved.

In order to further verify these stresses, the resulting reaction force on the torque arm was compared to the forces applied to the model. The total weight of the reducer (–11,929 N), coupling box (–7,573.3 N) and motor (–23,583.2 N) in the Y-direction gave a reaction force on the torque arm in the Y-direction of + 43,085.5 N. Applying the SFy = 0 gives the same result, and the model is consistent.

Dynamic analysis. *PTC Pro/Mechanica* was also used to perform the dynamic analyses. Dynamic analysis measures a system's response to a number of time-driven loads. In particular, dynamic random analysis was used. Dynamic random analysis measures the response of a system to a power spectral density function (PSD) (Refs. 16–17). The load input is a force or acceleration PSD given over a range of frequencies. In order to conduct a dynamic analysis, a modal analysis must first be run. A modal analysis calculates the frequencies of failure (Refs. 18–20).

To ascertain the validity of both the assumptions and the calculations, acceleration versus frequency data was collected in three different planes, and in various locations from the prototype of the alignment-free drive. A magnetic probe and machinery health analyzer were connected to the prototype to acquire this information. Figure 9 shows the acceleration versus frequency in graphical form from the readings taken from the prototype.

The modes of failure acquired during the prototype test were very close to those calculated in the modal analysis, and further verified the accuracy of our analysis which can be seen

continued

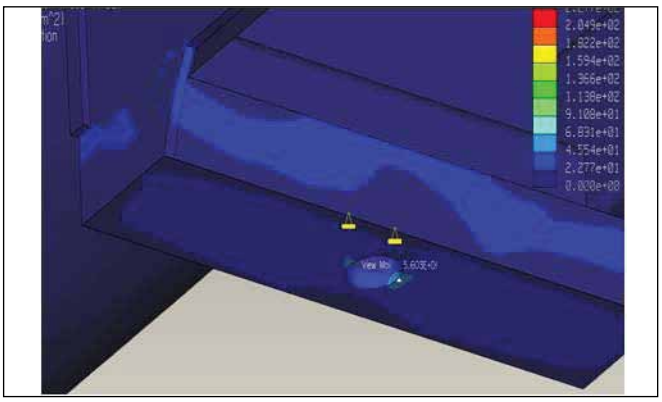

Figure 8—Extended bar stress field.

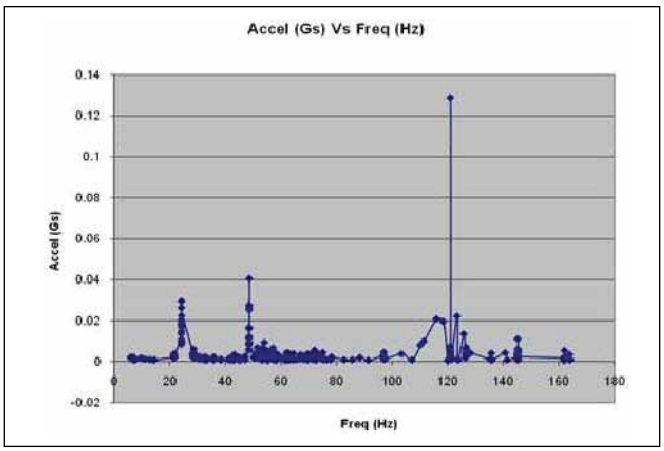

Figure 9—Acceleration versus frequency graph.

in Table 1.

The results in Table 1 show that the error in the analysis is comparable to the error computed according to (Ref. 13). Since the FEA model was extremely large, there was a larger window of acceptable error.

The acceleration versus frequency tables were also used as inputs in the dynamic random analysis to show how the system responded to various frequencies. The model was constrained—as shown in Figure 7b—and the loads were applied in a similar fashion as the static analysis, except that for the dynamic random analysis, the PSD data was used as the input to the analysis. Figure 10a shows one of the internal, structural tubing members. This member showed the maximum stress of the entire system. The resulting maximum stress on the internal structural tubing was 450 MPa. This stress, however, was over a small area and can be disregarded due to a singularity region at that point. The realistic stress was around 300 MPa.

Figure 10b shows the stress distribution on the motor adapter front plate. This is the location where the adapter is bolted to the reducer. This area also showed stresses near 300 MPa under dynamic loading. From these results, it is clear that there was a significant reduction in stress on the motor adapter with the new design. The reducer housing and the motor adapter will not fail under running loads.

Based on the FEA research results, optimization proposals are made to increase the structural integrity of the alignment-free drive and reduce the chance of failure. The suggestions are:

Modify the four (top and bottom) bottom mounting bars so that they extend the full length of the motor adapter. This allows for a greater load distribution of the reaction forces caused by the fixed torque arm. This larger contact area will not cause high stresses on the internal structural tubing. This becomes even more important as the design is applied to larger capacity reducers, couplings and motors. These extended bars can also be used as a skid-pad that will aid in transportation and will also allow the reducer to sit on the ground, if need be.

The analyses shown are for the case where the external torque load is applied in the counterclockwise direction to the output shaft, and drive is constrained in the torque arm position nearest to the reducer location No. 1. In this case, the motor adapter and the entire motor act as a cantilever beam extending from that torque arm position. Since the majority of the weight of the drive system is due to the motor, there are significantly higher stresses on the reducer and motor adapter interface and bottom torque arm location pad. Since both torque arm positions 1 and 2 shown in Figure 3 are valid configurations for the drive, it is suggested that when space and application allow, put the torque arm at the position nearest the motor. This effectively shortens the moment arm caused by the cantilevered motor, and also puts the center of gravity of the system above the constraint.

When the drive system was analyzed with the external torque acting in the clockwise direction, the stress results were much smaller than when it acted in the counterclockwise direction. That is because this torque will effectively subtract from the moment created from the weight of the motor acting at a large distance from the torque arm because they are acting in opposite directions. Again, when space and application allow, orienting the output shaft so that it is driving in the clockwise direction will significantly lower stress and decrease the chance of failure.

Table 1-Comparison of Frequency

Mode	Estimated	Experimental	%
	(Hz)	(Hz)	error
1	28.3	24.9	12.0
2	51.1	48.6	4.9
3	137.8	121.8	11.6

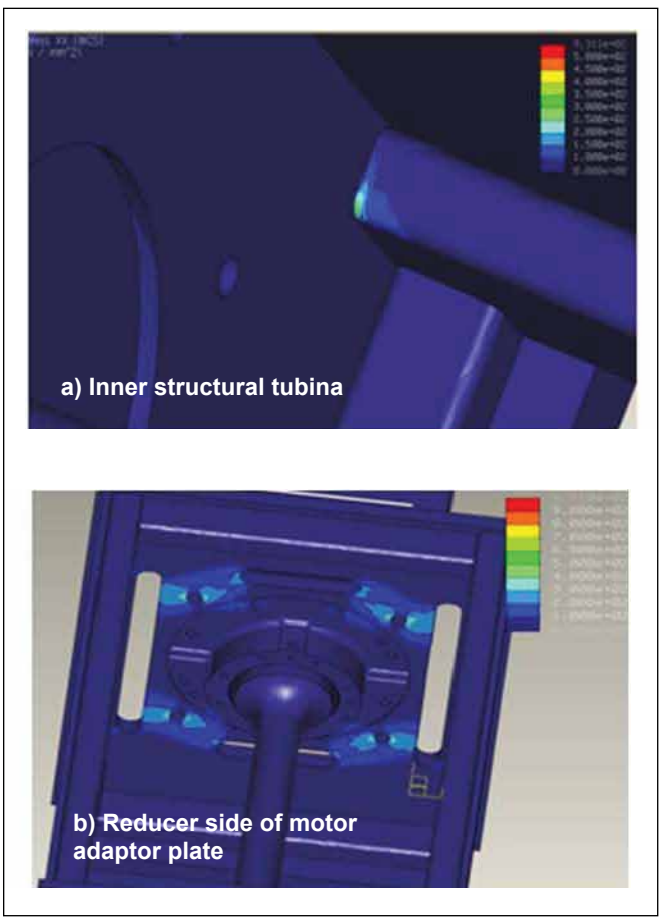

Figure 10—Dynamic, random analysis stress distribution.

Conclusion

The failure of gear reducer housing units is directly related to the combination of both static and dynamic loadings. High stresses arise in the gear reducer housing from both the large sizes of the components, improper gear meshing and impact, and from vibrations coming from the system. FEA analysis showed the stress areas that would cause failure. The failure would begin by localized yielding of the structural tubing at the mounting hole and propagate along the length of the tubing. These areas were looked at more closely.

The redesigned size of the bottom bar had a significant effect on the maximum stress experienced on the structural tubing and the area surrounding it. The data collected from the prototype helped us verify the FEA and show that the redesign of the bottom bar would be sufficient to reduce the stresses and prevent failure of the alignment-free gear reducer housing system.

References

1. Broker-Kornowske, V.J., T.R. Grimm and G.L. Viegelahn. Finite Element and Experimental Analysis of a Speed Reducer Housing, 1988: p. 137–143.
2. Maslov, I.V., R. McCafferty and J.P. Rea. Finite Element Analysis of Dynamic Rigidity of Diesel Engine Housing, 1995. Boston, MA, ASME.
3. Wang, W.L., FEA-Based Structure Optimization for the Drive End Housing of an Automotive Starter, 2008. Piscataway, NJ, USA: IEEE.
4. Bosco, Jr. R., et al. "Finite Element Analysis of a Compressor Housing Used in High-Pressure Refrigeration System," 2008, San Antonio, TX, American Society of Mechanical Engineers.
5. Levecque, N., et al. "Model and Experiment for Vibration Reduction of a Single-Cylinder Reciprocating Compressor," 2008, Exeter, United Kingdom, Chandos Publishing.
6. Vinayak, H. and R. Singh. "Multi-body Dynamics and Modal Analysis of Compliant Gear Bodies," *Journal of Sound and Vibration*, 1998, 210 (2): p. 171–212.
7. Kubur, M., et al. "Dynamic Analysis of Multi-Mesh Helical Gear Sets by Finite Elements," 2003, Chicago, IL. American Society of Mechanical Engineers.
8. Becene, A.T. "A Bracket Design Optimization in Random Vibration Environment with FEA and Robust Engineering Methods," 2001, Kissimmee, FL, Society for Experimental Mechanics, Inc.
9. Tanaka, E., et al. "Vibration and Sound Radiation Analysis for Designing a Low-Noise Gearbox with a Multi-Stage Helical Gear System," *JSME International Journal*, Series C (Mechanical Systems, Machine Elements and Manufacturing), 2003. 46 (3): p. 1178–85.
10. Choy, F.K., et al. "Modal Analysis of Multi-Stage Gear Systems Coupled with Gearbox Vibrations," *Journal of Mechanical Design*–Transactions of the ASME, 1992. 114 (3): p. 486–497.
11. Morey, J.A. "Turbo-Compressor Vibration Reduction using Vibration, Modal and Finite Element Analysis," 1987, Barton, Australia, Institute of Engineers.
12. Ganz, K. and M. ller. "Structural Mechanics Analysis of Gear Unit Components in the Development Process Using the Finite Element Method," VDI Berichte, 2005 (1904 I): p. 247–268.
13. Jingshu,W., et al. "Vibration Analysis of Medical Devices with a Calibrated FEA Model," Computers Structures, 2002. 80 (12): p. 1081–6.
14. Gabbert, U., M. Zehn and F. Wahl. "Improved Results in Structural Dynamic Calculations by Linking FEA and Experimental Modal Analysis (EMA)," 1995, Boston, MA.
15. Ye, Z., et al. "Structure Dynamic Analysis of a Horizontal-Axis Wind Turbine System using a Modal Analysis Method," *Wind Engineering*, 2001, 25 (4): p. 237–48.
16. Braccesi, C., et al. "Fatigue Behavior Analysis of Mechanical Components Subject to Random Bimodal Stress Process: Frequency Domain Approach," *International Journal of Fatigue*, 2005, 27 (4): p. 335–345.
17. Hu, J.M. "Life Prediction and Damage Acceleration Based on the Power Spectral Density of Random Vibration," *Journal of the IES*, 1995, 38 (1): p. 34–40.
18. Lee, Y.S., H.S. Kim and C.H. Han. "A Study on the Vibrational Characteristics of the Continuous Circular Cylindrical Shell with the Multiple Supports Using the Experimental Modal Analysis," Key Engineering Materials, 2006, 236–328: p. 1617–20.
19. Liu, H., F. Bai and J.L. Gobeli. "FEA Modeling and Modal Pushover Analysis of a 14-Story Office Building in Anchorage, Alaska," 2006, St. Louis, MO, American Society of Civil Engineers.
20. Li-gang, Q. and W. Da-wei. "Strength and Modal Analysis of Welded Bracket of the Large-Scale Agitator," Key Engineering Materials, 2007, p. 1485–8.

Paul F. Martin *is chief applications engineer with Sumitomo Machinery Corporation of America. Paul received his BS Degree in Mining Engineering from the Colorado School of Mines in 1979. He has more than 30 years of experience specializing in mining equipment and bulk material handling, focusing on product sales, engineering applications, product development, project and contract management, equipment feasibility studies and mine planning. He has co-authored numerous papers relative to mining equipment and is "inventor" for patents related to walking draglines.*

Charles Ritinski *is the ESC Engineer with Sumitomo Machinery Corporation of America. Charles has held a wide variety of positions over the course of more than three decades in the power transmission industry, including engineering, research and development, product management, field service, marketing and sales positions. Charles was instrumental in the development of more than a dozen types of product improvements. His BS Degree is from the Pennsylvania Sate University.*